JOURNAL OF SOLID STATE CHEMISTRY 73, 338–347 (1988)

# Lithium Intercalation in $Ln_{1/3}NbO_3$ Perovskite-Type Phases ($Ln$ = La, Nd)

A. NADIRI, G. LE FLEM, AND C. DELMAS

*Laboratoire de Chimie du Solide du CNRS, Université de Bordeaux I, 351, cours de la Libération, 33405 Talence Cedex, France*

Received April 8, 1987

Lithium can be intercalated either chemically or electrochemically in $Ln_{1/3}NbO_3$ perovskite-type phases ($Ln$ = La,Nd). In the starting material the electrostatic repulsion between rare earth ions leads to relative ordering within the $NbO_3$ network. Every other plane of perovskite cavities contains rare earths. The related formula is $\square_{1/2}(Ln_{1/3}\square'_{1/6})NbO_3$. In both systems, solid solutions are observed in the first part of the intercalation reaction. While almost all perovskite cavities are filled in the neodymium phases, the higher ionic character of the La–O bonds prevents practically the $\square'$ sites from Li intercalation. For the highest intercalation rates which attain 0.80, a new site is involved. The physical properties of the intercalated materials have been described in connection with the electrochemical behavior. Whatever the intercalation rate, the *d* electrons remain localized and the electronic behavior is characterized by a hopping mechanism. 1988 Academic Press, Inc.

## Introduction

In the scope of the investigations devoted to alkali metal intercalation reactions (*1–3*) interest has been shown in the recent years to studies of 3D-skeleton materials, especially of perovskite-derived structures.

Intercalation reactions have been carried out in two main classes of materials:

(i) strictly corner sharing structures like $WO_3$ (*5, 6*), $ReO_3$ (7–9), or tungsten bronzes (*10, 11*);

(ii) $ReO_3$ crystallographic shear plane structures (with simultaneous corner and edge sharing) such as $TiO_2$(B) (*1, 2*) $VO_2$(B) (*13*), $V_6O_{13}$ (*14*) and $FeV_3O_8$ (*7, 9, 15*).

In the first group of materials the relative flexibility of the structures allows octahedra rotations without framework bond breaking during the intercalation processes. In $Li_{0.36}WO_3$ for instance the $WO_6$ octahedra tilting leads to two unequivalent alkali metal sites respectively 4 and 12 coordinated (*6*). From $ReO_3$ Murphy *et al.* have obtained ilmenite-related phases, $LiReO_3$ and $Li_2ReO_3$ (*7, 8*). In this case the octahedra twisting converts the perovskite 12-coordinated cavity into two face sharing octahedra.

In the $ReO_3$ crystallographic shear plane structures the edge sharing makes $MO_6$ twisting difficult during lithium intercalation and the framework is practically not modified.

It has been shown recently that lithium ions can be incorporated in the lattice of the $Ln_{1/3}NbO_3$ rare earth perovskite-derived structure by a coupled substitution formally

0022-4596/88 $3.00

of type $Nb^{5+} = Li^+ + Ti^{4+}$ (*16*). The materials have been characterized from the crystallographic point of view. The perovskite framework is maintained for small insertion rates, while an aeschynite-type phase (derived by crystallographic shearing from the perovskite structure) is observed for larger $x$-values. The lithium mobility has been determined by impedance measurements and NMR spectroscopy (*17*).

Preliminary work has also shown that lithium can be electrochemically intercalated in $Nd_{1/3}NbO_3$ (*16*).

This paper describes lithium intercalation in both $La_{1/3}NbO_3$ and $Nd_{1/3}NbO_3$. These materials can be considered as intermediate between the two previously reported types of structures. The $NbO_3$ framework is made up of $NbO_6$ corner sharing octahedra, the structure being stabilized by the rare earth ions inserted in the perovskite A cavities. These phases can be compared to $La_{0.14}WO_3$ (*6*) where the lanthanum ions are randomly distributed over the same 12-coordinated sites, whereas relative ordering exists in the niobate structure (*18, 19*).

## Structure Description

The $Ln_{1/3}NbO_3$ structure shown in Fig. 1 has been described by P. N. Iyer and A. J. Smith (*18*). The rare earth ions are partially ordered within the 3D-$NbO_3$ network. In the representation given in Fig. 1, the centers of the 12-coordinated perovskite cavities form planes at $z = 0$ and $z = \frac{1}{2}$. Two-thirds of the $z = 0$ sites are randomly occupied by rare earth atoms, whereas the $z = \frac{1}{2}$ sites are empty. Such a distribution leads to doubling of the $c$-parameter of the cubic perovskite-type cell, so that a tetragonal symmetry could be expected. In fact a small orthorhombic distortion occurs: $a_{orth} \simeq a_{cub}$; $b_{orth} \simeq a_{cub}$; $c_{orth} \simeq 2a_{cub}$. Vacancies at $z = \frac{1}{2}$ lead to opposite shifts of the niobium ($z = 0.262$) and oxygen ($z = 0.226$) atoms from their ideal positions ($z = 0.25$). Off-centering of $Nb^{5+}$ leads to alternating short and long Nb–O bonds along the $c$-axis.

## Experimental

### (*a*) *Starting Phase Preparation*: $Ln_{1/3}NbO_3$ (*Ln* = *La, Nd*)

These materials are obtained by direct synthesis from stoichiometric amounts of the binary oxides $Ln_2O_3$ and $Nb_2O_5$. Pellets of the starting mixture undergo three 20-hr thermal treatments, respectively, at 1200, 1300, and finally 1350°C. Resulting powder

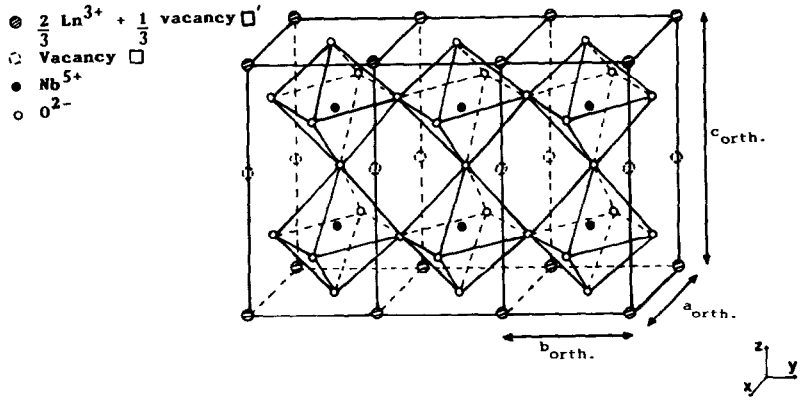


FIG. 1. Structure of $Ln_{1/3}NbO_3$ phases.

materials are white ($Ln$ = La) or purple ($Ln$ = Nd).

*(b) Intercalation Reactions*

Lithium intercalation reactions were achieved both electrochemically and chemically with organometallic reagents. Intermediate Li compositions were obtained by the "chemical short circuit method" recently developed in this laboratory (*20*). For each example special attention must be paid to grinding of the starting material: as a matter of fact, lithium intercalation can be limited for large size grains by the reaction kinetics.

*Electrochemical Intercalation*

The following electrochemical chain has been used:

$$Li/LiClO_4 \text{ in } PC/Ln_{1/3}NbO_3 + \text{graphite}.$$

To ensure a macroscopic electronic conductivity, graphite representing 30% in weight has been added to the positive electrode. All the discharge–charge processes are assured galvanostatically. They are monitored by a real time–time slicing HP1000 A600 computer (*21*). To obtain the thermodynamic emf vs composition curves, relaxation periods are allowed until constant voltage values are found. After the electro-chemical reaction the positive electrode material is recovered, washed with hexane, dried under vacuum, and then characterized by X-ray diffraction using the Guinier technique.

*Chemical Intercalation*

Large amounts of lithium intercalated compounds were obtained using solutions of *n*-butyllithium in hexane or lithium naphthalide in THF. While the former reagent allows materials with potentials equal to 1.0 V vs $Li/Li^+$ electrode to be obtained, very reductive phases can be obtained with the latter one, as its potential is lower than 0.5 V vs $Li/Li^+$ (*22*). This reagent is obtained by dissolution of lithium in a solution of naphthalide in THF (*23*).

Deintercalation reactions were done to test the reversibility of the reactions using iodine as oxidation medium.

*Chemical Short Circuit Method*

This method has been used to obtain large amounts of intercalated phases with intermediate compositions. It requires mixing of two phases with different intercalation rates. As a matter of fact, the nonintercalated starting phase is mixed with an intercalated phase previously synthesized. To enhance the reaction speed the mixture is wetted with a liquid electrolyte and then pelletized to ensure a good contact for electronic mobility. The resulting mixture can be considered as a rocking chair-battery in short circuit and the following reaction occurs:

$$a\langle H\rangle + Li_{x_1}\langle H\rangle \rightarrow (a+1)Li_{x_1/(a+1)}\langle H\rangle$$

More generally the nonintercalated phase $\langle H\rangle$ can be replaced by a partially intercalated one, $Li_{x_0}\langle H\rangle$.

When equilibrium is reached, an electrochemical cell is built, with a small fraction used to check its potential vs the lithium electrode and to compare with the thermodynamic emf curves.

In the present research this method has been utilized to obtain easily phases only slightly intercalated for optical studies.

## Results

*(a) Electrochemical Intercalation*

The cell voltage variations vs composition under constant current density are represented on Figs. 2 and 3 for the two $Li//Li_xLn_{1/3}NbO_3$ systems. The behavior of the cells clearly shows the reversibility of the intercalation reactions.

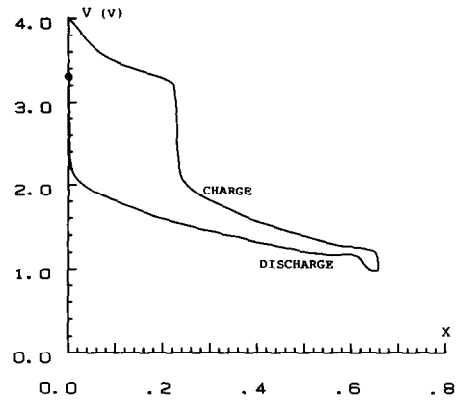


FIG. 2. Cell voltage variation vs Li rate in a Li// $Li_xLa_{1/3}NbO_3$ cell ($J$ = 50 $\mu$A/cm$^2$).

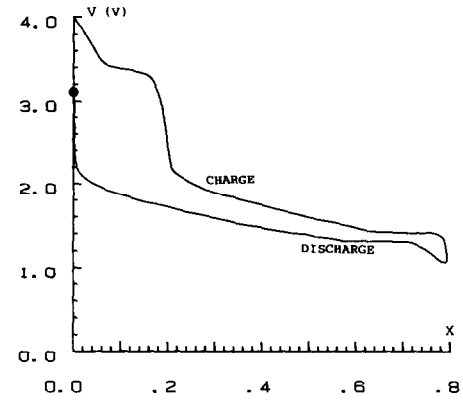


FIG. 3. Cell voltage variation vs Li rate in a Li// $Li_xNd_{1/3}NbO_3$ cell ($J$ = 50 $\mu$A/cm$^2$).

Thermodynamic emf vs composition curves are plotted in Fig. 4. In both systems a solid solution with upper limit $x = 0.53$ ($Ln$ = La) and $x = 0.64$ ($Ln$ = Nd) has been found. This phase is in equilibrium during a further discharge process with a second phase corresponding to $x = 0.80$). While the discharge and the thermodynamic curves are quite similar for $x > 0.1$, a strong difference is observed for the small intercalation rates.

*(b) Chemical Intercalation*

$Li_xLa_{1/3}NbO_3$ phases were also obtained by this method. An excess of *n*-butyllithium allows the composition $Li_{0.53}La_{1/3}NbO_3$ to be obtained, while a formulation $Li_{0.80}La_{1/3}NbO_3$ can be reached with the lithium naphthalide solution. The composition of these materials has been checked by chemical analysis.

Electrochemical cells were built up from the lithium intercalates to corroborate the above results. The starting ocv values and the shape of the charge and discharge curves confirm the complete analogy between chemical and electrochemical intercalation.

A lithium deintercalation reaction from $Li_{0.80}La_{1/3}NbO_3$ using iodine dissolved in $CH_3CN$ leads to composition $Li_{0.04}La_{1/3}NbO_3$. Afterward to prove the complete reaction reversibility the latter material has been electrochemically reintercalated.

All these results have been obtained using $La_{1/3}NbO_3$ of approximately 1 $\mu$m grain size. If materials with larger grains (~10 $\mu$m) are used, the intercalation with *n*-butyllithium seems to be more restricted. After a 1-week reaction an overall $x = 0.22$ value has been obtained as intercalation limit, even if a large excess of *n*-butyllithium is used.

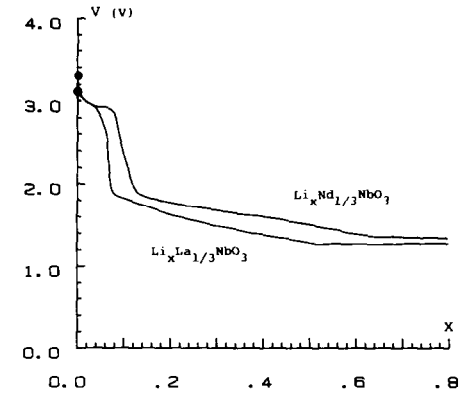


FIG. 4. Variation of the thermodynamic potential (ocv) vs Li rate for Li//$Li_xLn_{1/3}NbO_3$ cells ($Ln$ = La and Nd).

TABLE I

UNIT CELL PARAMETERS OF THE $Li_xLa_{1/3}NbO_3$ PHASES

| | $Li_xLa_{1/3}NbO_3$ | | | |
|---|---|---|---|---|
| | $0 \leq x \leq 0.07$ | $x = 0.22$ | $x = 0.53$ | $x = 0.80$ |
| $a$(Å) ± 0.003 Å | 3.907 | 3.917 | 3.921 | 3.918 |
| $b$(Å) ± 0.003 Å | 3.919 | 3.917 | 3.921 | 3.918 |
| $c$(Å) ± 0.005 Å | 7.901 | 7.909 | 7.911 | 7.900 |
| $V$(Å$^3$) ± 0.3 Å$^3$ | 120.9 | 121.3 | 121.6 | 121.3 |
| $c/a$ ± 0.003 | 2.022 | 2.019 | 2.017 | 2.016 |

*(c) Cell Parameter Variation*

Tables I and II display the unit cell parameter of the $Li_xLn_{1/3}NbO_3$ phases. Results obtained by the various intercalation methods are idential.

The X-ray diffraction patterns of all intercalated phases have been indexed in an orthorhombic system similar to that of the starting phases with space group $P_{mmm}$. For all samples with $x > x_L^{Ln}$ ($x_L^{La} = 0.07$, $x_L^{Nd} = 0.10$) splitting between $(hkl)$ and $(khl)$ lines disappears, apparently giving evidence of a tetragonal unit cell. Nevertheless, from powder diffraction patterns, it is impossible to draw unambiguous conclusions. For the lower intercalation values ($x < x_L^{Ln}$), corresponding to the first part of the ocv curve, no significant modification of the X-ray diffraction pattern can be detected.

TABLE II

UNIT CELL PARAMETERS OF THE $Li_xNd_{1/3}NbO_3$ PHASES

| | $Li_xNd_{1/3}NbO_3$ | | |
|---|---|---|---|
| | $0 \leq x \leq 0.10$ | $x = 0.64$ | $x = 0.80$ |
| $a$(Å) ± 0.003 Å | 3.902 | 3.909 | 3.912 |
| $b$(Å) ± 0.003 Å | 3.916 | 3.909 | 3.912 |
| $c$(Å) ± 0.005 Å | 7.766 | 7.811 | 7.828 |
| $V$(Å$^3$) ± 0.3 Å$^3$ | 118.7 | 119.3 | 119.8 |
| $c/a$ ± 0.003 | 1.990 | 1.998 | 2.001 |

*(d) Electronic Conductivity*

Niobium(V) is reduced during the lithium intercalation. The ESR spectrum obtained at 4.2 K for the $Li_{0.015}La_{1/3}NbO_3$ composition shows unambiguously the existence of $Nb^{4+}$ ions with a $g$-factor of 1.81.

In all cells, graphite must be added to the positive electrode material to ensure a sufficient electronic conductivity. Such a requirement clearly shows the low electronic conductivity of the intercalated perovskites even for high lithium content ($x \simeq 0.80$).

The electronic conductivity has been determined by the four probe technique. That of the starting phase $La_{1/3}NbO_3$ is very low, i.e., smaller than $10^{-10}$ $\Omega^{-1}$ cm$^{-1}$ at 20°C. Figure 5 shows a plot of log $\sigma$ vs reciprocal

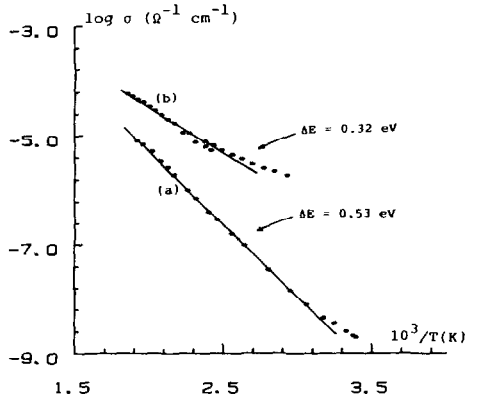


FIG. 5. Variation of the conductivity vs reciprocal temperature for $Li_{0.22}La_{1/3}NbO_3$ (a) and $Li_{0.80}La_{1/3}NbO_3$ (b).

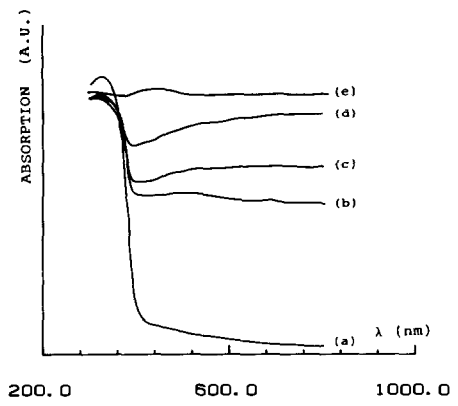


FIG. 6. Diffuse reflectance spectra for $Li_xLa_{1/3}NbO_3$ phases for (a) $x = 0$, (b) $x = 0.005$, (c) $x = 0.010$, (d) $x = 0.015$, and (e) $x = 0.070$.

temperature for the $x = 0.22$ and $x = 0.80$ $Li_xLa_{1/3}NbO_3$ phases.

*(e) Diffuse Reflectance*

An optical investigation has been realized by recording the diffuse reflectance spectra in the UV and visible regions for several compositions (Fig. 6). The gap determined for $x = 0$ (Eg = 3.1 eV), in good agreement with that observed for $Nb_2O_5$ (Eg = 2.92 eV) characterizes an $O^{2-} \rightarrow Nb^{5+}$ electronic charge transfer. It holds for slightly intercalated phases, while an absorption, almost constant along the explored wavelength domain and which characterizes a hopping phenomenon, increases with the intercalation rate. This behavior is emphasized by the observed color changes: The starting phase $La_{1/3}NbO_3$ is white. Slightly intercalated niobates are gray blue and become darker with increasing intercalation rate and even black for $x > 0.07$.

## Discussion

*(a) Electrochemical Behavior*

This investigation shows clearly that the 3D-network remains unchanged even for high intercalation amounts. The intercalation reaction exhibit a good reversibility, as shown by Figs. 2 and 3 as well as by iodine deintercalation. The strong polarization which appears at the end of the charge process ($x \simeq 0.2$) arises from the formation of a thin skin of $Ln_{1/3}NbO_3$ which is insulating from both ionic and electronic points of view.

An interesting feature to discuss is the cell voltage difference observed in comparing the behavior of the lanthanum and neodymium phases (Fig. 4). The higher voltage observed for the neodymium niobate cells results from a higher oxidizing character of niobium in this phase than in the lanthanum phase. This behavior can be related to the more ionic character of the La–O bond which enhances the covalency of the niobium–oxygen bond and makes it more difficult to trap an extra electron on the niobium atom. On the contrary, the lower energy of the niobium level increases the oxidation rate of $Nd_{1/3}NbO_3$.

It is well known that the intercalation kinetics is directly connected to the grain size of the intercalated material. A small grain size increases the active intercalation surface area and simultaneously decreases the number of jumps required for the mobile ion to reach an equilibrium position in the grain bulk.

Intercalation with a large excess of *n*-butyllithium on large size grains of $La_{1/3}NbO_3$ leads to an overall composition close to $Li_{0.22}La_{1/3}NbO_3$ after 1 week reaction. As shown in Fig. 4 the open circuit voltage obtained for this composition (1.62 V) is very far from the *n*-butyllithium potential. One may infer that the material is not in equilibrium conditions at the end of the experiment. To illustrate this behavior an electrochemical cell was set up just after removing the sample from the organometallic solution. The variation of its open circuit voltage vs time plotted on Fig. 7 illustrates progressive relaxation of the material. At the begining the low potential value shows

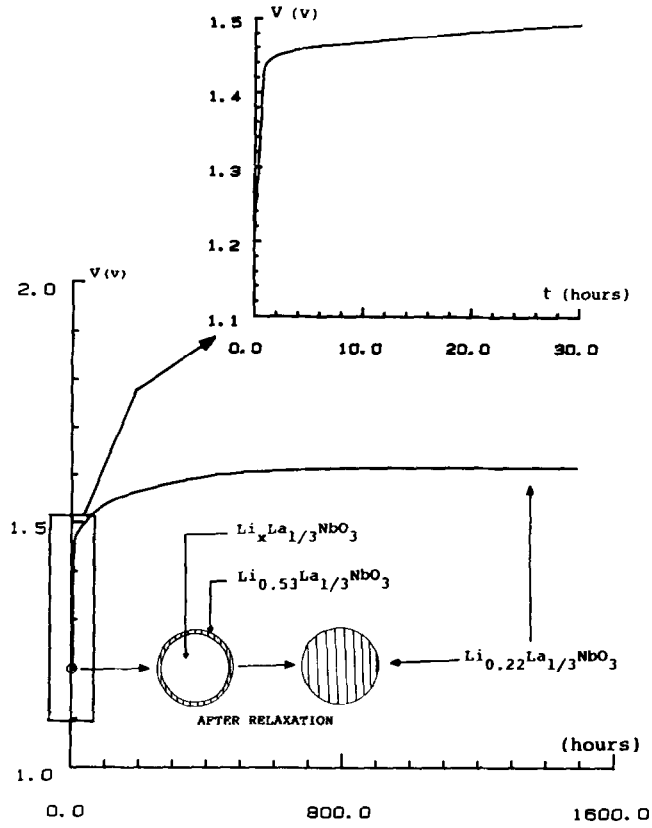


FIG. 7. Variation vs time of the open circuit voltage of a Li//$Li_{0.22}La_{1/3}NbO_3$ cell. The time origin has been taken when the material of overall composition $Li_{0.22}La_{1/3}NbO_3$ is removed from a *n*-butyllithium solution after 1 week contact.

the existence of a thin film of highly intercalated phase. Afterward $Li^+$ ions and electrons diffuse within the grain and the potential reaches its normal equilibrium value (1.62 V).

*(b) Crystal Chemistry*

As expected the presence of strong *Ln*–O bonds in the perovskite lattice hinders large rotations of skeleton octahedra such as those observed for $Li_xWO_3$ (*6*) or $LiReO_3$ and $Li_2ReO_3$ (*8*, *9*) phases.

Precise knowledge of the lithium distribution could require neutron diffraction investigations. These experiments are in progress for the $Li_{0.22}La_{1/3}NbO_3$ and $Li_{0.80}La_{1/3}NbO_3$ compositions. Nevertheless, from a close examination of the structure of the starting phase some reasonable hypotheses can be formulated. Figure 8 shows two adjacent perovskite-type cavities within the $NbO_3$ network. This representation has been deduced from the atomic positions published by P. N. Iyer and A. J. Smith (*18*). As discussed above, $Ln^{3+}$ ions are statistically distributed in the cavity planes situated at $z = 0$ and $z = 1$. Assuming as previously that the vacancies at $z = 0$ and $z = \frac{1}{2}$ are, respectively, labeled as $\square'$ and $\square$, the formula of the unintercalated niobate can be written $\square_{1/2}(Ln_{1/3}\square'_{1/6})NbO_3$. As $\square$ is surrounded by a smaller

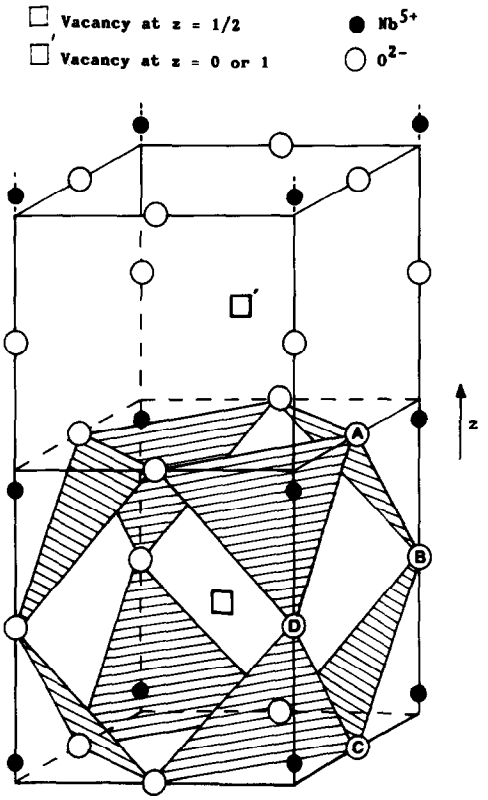


FIG. 8. Drawing of two adjacent cavities in the $Ln_{1/3}NbO_3$ lattices.

number of $Ln^{3+}$ than □′ (Fig. 1), this site can be more easily filled by $Li^+$ ions from an electrostatic point of view. As a result the $x = 0.50$ value is only slightly exceeded for lanthanum niobate ($x \simeq 0.53$). On the contrary, in neodymium niobate the lower ionic character of the Nd–O bond decreases the lithium–neodymium repulsion and allows easier lithium intercalation in the rare earth surrounded, □′ site (leading to $x \simeq 0.64$).

In both systems the plateau observed in the final part of the discharge curve shows the presence of a two phase domain limited by the $x = 0.80$ composition. As an $x$ value larger than $\frac{2}{3}$ is observed, a new lithium site must be involved.

Taking into account the lithium ion size, a close examination of the perovskite cavity located at $z = \frac{1}{2}$ shows that it is possible to introduce two $Li^+$ ions in the same cavity. But such a distribution would lead indeed to very large $Li^+$–$Li^+$ repulsions. As a result this hypothesis must be rejected.

Another position can be considered: the center of each bottleneck of the A-type tunnels situated at $z = \frac{1}{2}$ (bottleneck ABCD, for example, in Fig. 8). Although such a position is unusual for lithium, it can be considered as it leads to realistic Li–O bond lengths (1.96 and 2.17 Å) and large Li–Li distances (3.91 and 4.33 Å). The total occupancy of this site would correspond to one $Li^+$ ion per $La_{1/3}NbO_3$ unit.

Such a square planar Li environment already has been detected in $Li_{0.20}ReO_3$, $Li_{0.36}WO_3$, and $Li(Cu_{3-x}Li_x)$ $[Ti_{3-x}M_{1+x}]O_{12}$ ($M$ = Nb,Ta) phases with perovskite-like structures (*6, 24, 25*). In those materials the square planar environment results from new sites which appear in the $ReO_3$ framework as a result of large octahedra tilting. In the present case, occurrence of rare earth atoms in the perovskite cavity hinders such a large tilting and the pseudosquare sites occupied by extra $Li^+$ ions would be therefore, simply, the bottleneck between the A cavities of the perovskite structure.

This hypothesis has to be checked indeed by neutron diffraction.

### (c) *The Slightly Intercalated Materials*

Electronic conductivity and optical study of $Li_xLa_{1/3}NbO_3$ ($x \geq 0.07$) clearly show the semiconducting character of this material. This behavior is characteristic of a hopping phenomenon. It seems that the number of intercalated electrons on one hand, and the $Nb^{4+}$ 4*d* shells extension and their overlapping with oxygen $p\pi$ orbitals on the other hand are too small to lead to an electron delocalization as observed in some tungsten bronzes (*26*).

Furthermore, for small amounts of inter-

calation another phenomenon seems to exist, as suggested in both systems by the high voltage values observed (Fig. 4). These values are very close to the open circuit voltage values obtained for unintercalated niobate: 3.27 V for $Li//La_{1/3}NbO_3$ and 3.10 V for $Li//Nd_{1/3}NbO_3$.

In addition, two other results should be pointed out from the structural point of view:

(i) The ESR signal observed for $Li_{0.015}La_{1/3}NbO_3$ is wide (400 G). Moreover, the expected hyperfine structure characterizing the isolated $Nb^{4+}$ ion has never been detected as, for instance, in the Nasicon-type related phosphate $Na_4Nb(PO_4)_3$ when doped with $Nb^{4+}$ (*27*). This behavior could suggest $Nb^{4+}$–$Nb^{4+}$ interactions.

(ii) The diffuse reflectance spectrum obtained for very slightly intercalated phases ($0.005 \leq x \leq 0.015$) does not show the expected absorption band characteristic of free $Nb^{4+}$ ions (*28, 29*), but rather shows simple overlapping of a constant absorption over the whole explored wavelength domain, due to hopping phenomena, and the $O^{=} \rightarrow Nb^{5+}$ charge transfer band situated at 3.1 eV.

All these features are consistent with the presence of small clusters of reduced niobium within crystallites of global composition close to that of the starting $Ln_{1/3}NbO_3$ phase.

For these compositions the open circuit voltage of the cells remain in the vicinity of those of unintercalated niobates (Fig. 4).

Of course these clusters are too small to be detected by X-ray diffraction and the diffraction spectrum remains identical to that of the starting material. It should be noted that no line broadening has been observed for these compositions. For the overall lithium rates $x = 0.07$ ($Ln$ = La) and $x = 0.10$ ($Ln$ = Nd) the clusters probably percolate and a classical disordered solid solution is then obtained, as shown by the modification of the cell voltage values (Fig. 4) and the change in the unit cell parameters.

## References


1. M. S. WHITTINGHAM, *Prog. Solid State Chem.* **12,** 41 (1978).
2. P. HAGENMULLER AND W. VAN GOOL, "Solid Electrolytes," Academic Press, New York/London (1978).
3. J. ROUXEL, *in* "Intercalated Layer Materials" (F. A. Levy, Ed.), Reidel, Dordrecht (1979).
4. M. S. WHITTINGHAM AND A. J. JACONSON, "Intercalation Chemistry," Academic Press, New York (1982).
5. K. H. CHENG AND M. S. WHITTINGHAM, *Solid State Ionics* **1,** 151 (1980).
6. P. J. WISEMAN AND P. G. DICKENS, *J. Solid State Chem.* **17,** 91 (1976).
7. D. W. MURPHY, M. GREENBLATT, R. J. CAVA, AND S. M. ZAHURAK, *Solid State Ionics* **5,** 327 (1981).
8. R. J. CAVA, A. SANTORO, D. W. MURPHY, S. ZAHURAK, AND R. S. ROTH, *J. Solid State Chem.* **42,** 251 (1982).
9. R. J. CAVA, A. SANTORO, D. W. MURPHY, S. ZAHURAK, AND R. S. ROTH, *Solid State Ionics* **5,** 323 (1981).
10. I. D. RAISTRICK, A. J. MARK, AND R. A. HUGGINS, *Solid State Ionics* **5,** 351 (1981).
11. I. D. RAISTRICK, *Solid State Ionics* **9/10,** 425 (1983).
12. R. MARCHAND, L. BROHAN, AND M. TOURNOUX, *Mat. Res. Bull.* **15,** 1291 (1980).
13. B. ZACHAU-CHRISTIANSEN, K. WEST, AND T. JACOBSEN, *Mat. Res. Bull.* **20,** 485 (1985).
14. D. W. MURPHY, P. A. CHRISTIAN, F. J. DI SALVO, AND J. N. CARIDES, *J. Electrochem. Soc.* **126,** 497 (1979).
15. R. J. CAVA, A. SANTORO, D. W. MURPHY, S. ZAHURAT, AND R. S. ROTH, *J. Solid State Chem.* **48,** 309 (1983).
16. D. CONTE, Thesis, University of Bordeaux (1983).
17. L. LATIE, G. VILLENEUVE, D. CONTE, AND G. LE FLEM, *J. Solid State Chem.* **51,** 293 (1984).
18. P. N. IYER AND A. J. SMITH, *Acta Crystallogr.* **23,** 740 (1967).
19. V. K. TROUNOV, L. N. KOVBA, AND N. S. AFONCKII, *Vestik. Moskolsskovo Yniversiteta* **1,** 55 (1968).
20. C. DELMAS AND A. NADIRI, *Mat. Res. Bull.*, to be published.
21. A. MENDIBOURE AND C. DELMAS, *Comp. Chem.* **11**(3), 153 (1987).

22. D. W. MURPHY AND P. A. CHRISTIAN, *Science* **205,** 651 (1979).
23. R. T. ARNOLD AND S. T. KVLENOVIC, *Synth. Commun.* **7,** 223 (1977).
24. R. J. CAVA, A. SANTORO, D. W. MURPHY, S. M. ZAHURAK, AND R. S. ROTH, *J. Solid State Chem.* **50,** 121 (1983).
25. P. MOURON AND J. CHOISNET, *J. Solid State Chem.* **66,** 311 (1987).
26. J. B. GOODENOUGH, "Metallic Oxides," Pergamon, Elmsford, NY (1971).
27. A. EL JAZOULI, C. PARENT, J. M. DANCE, AND G. LE FLEM, *C. R. Acad. Sci.* **303,** 1005 (1986).
28. J. L. KETCHUM, K. L. SWEENEY, L. E. HALLIBURTON, AND A. F. ARMINGTON, *Phys. Lett. A* **94**(9), 450 (1983).
29. J. L. SWEENEY AND L. E. HALLIBURTON, *Appl. Phys. Lett.* **43**(4), 336 (1983).